Annals of the Academy of Romanian Scientists
Series on Physics and Chemistry Sciences
ISSN 2559-1061 Volume **4**, Number **2**/**2019**

SYNTHESIS OF PHOTOCATALYSTS BASED ON GRAPHENE OXIDE AND Fe_3O_4

Adrian Ionut NICOARA[1], Alexa CROITORU[2], Ovidiu OPREA[3], IONELA ANDREEA NEACSU[4], Ecaterina ANDRONESCU[5]

Abstract. *Organic synthetic dyes that are used by the textile industry, due to their high stability, lead to harmful effects for humans and animals using polluted water sources. Most dyes widely used, such as methylene blue, bromphenol blue or other phenolic compounds, when discharged into the environment in greater amounts, can cause serious contamination of the water sources they reach. Simple and fast systems are needed to help eliminate these drugs from the environment. Graphene is a material made up of a single layer of sp^2 hybridized carbon atoms, which has become one of the most researched materials ever since its discovery. Applications of graphene materials are variate, from solar cells to sensors, water treatment, and even cancer therapies. This study is focus on the preparation of GO@Fe_3O_4 composites with different morphologies and sizes, obtained by the precipitation method and used for environmental depollution.*
Keywords: nanocomposite, water treatment, graphene oxide, magnetite, separable photocatalysts.

1. Introduction

Environmental pollution is the main problem of the 21st century. Technological advancement and product diversification raise the problem of efficient recycling and elimination of the main pollutants in the environment. The pharmaceutical industry represents a pollution factor by introducing in the aquatic environment some traces of medicines of which the most common are antibiotics. Also, the textile industry produces a series of organic pollutants such as methylene blue [1]. This is a cationic dye known also as methylthioninium chloride used to impregnate the blue color of textiles. It can also be used in the pharmaceutical environment especially for veterinary use.

[1] PhD, Eng., Faculty of Applied Chemistry and Materials Science, University Politehnica of Bucharest, Romania, Academy of Romanian Scientists (adrian.nicoara@upb.ro).
[2] PhD student, Eng., Faculty of Applied Chemistry and Materials Science, University Politehnica of Bucharest, Romania, Academy of Romanian Scientists (croitoru.alexa@yahoo.com).
[3] Professor, PhD, Eng., Faculty of Applied Chemistry and Materials Science, University Politehnica of Bucharest, Romania (ovidiu.oprea@upb.ro).
[4] PhD, Eng., Faculty of Applied Chemistry and Materials Science, University Politehnica of Bucharest, Romania, Academy of Romanian Scientists (neacsu.a.ionela@gmail.com)
[5] Professor, PhD, Eng., Faculty of Applied Chemistry and Materials Science, University Politehnica of Bucharest, Romania, full member of the Academy of Romanian Scientists (ecaterina.andronescu@upb.ro)

Therefore, the elimination of this pollutant from the environment is an activity that has aroused, in recent years, the interest of the researchers [2–5]. The removal of colorants from wastewater has been studied using techniques such as: absorption [6,7], coagulation [8], chemical oxidation [9,10], electrochemical techniques and photocatalysis techniques [11–13]. The main disadvantage of using inorganic photocatalysts is that they can, in turn, become pollutants if not removed properly. That is why the actual need is to use materials that can combine photocatalytic properties with magnetic properties as an efficient solution.

Graphene is a material made up of a single layer of sp^2 hybridized carbon atoms, which has become one of the most researched materials ever since its discovery. Applications of graphene materials are diverse, from solar cells to sensors, water treatment, and even cancer therapies. Graphene can be successfully used as a support for magnetic nanoparticles, such as magnetite (Fe_3O_4).

Magnetite particles exhibit a reduced photocatalytic activity under sunlight, especially due to the high degree of agglomeration induced by the large specific surface and the magnetic interactions between these particles [14]. The incorporation of these nanoparticles into the graphene sheets is a promising solution to overcome this limitation, as it prevents the serious agglomeration of magnetite nanoparticles, which leads to high photocatalytic performance under sunlight by the contribution of improved photo-induced charge separation efficiency within the Fe_3O_4 nanoparticles.

This study is focused on the preparation of GO@Fe_3O_4 composites with different morphologies and sizes, obtained by the precipitation method and used for environmental depollution.

2. Materials and methods

2.1. Chemicals and reagents

In order to obtain magnetite nanoparticles, iron (II) sulfate heptahydrate ($FeSO_4 \cdot 7H_2O$), iron (III) chloride ($FeCl_3$) and ammonium hydroxide solution 25% (NH4OH) purchased from Merck (Sigma-Aldrich) were used.

The GO was obtained by Hummer's method [15][16]. Thus, 20 g of graphite were mixed with a concentrated solution of H_2SO_4 (60 mL), $K_2S_2O_8$ (10 g) and P_2O_5 (10 g) at 80 °C. The mixture was then allowed to cool to room temperature after which it was diluted with a large amount of water, filtered and washed until the filtrate reached neutral pH. The obtained powder was dried for 24 hours at 80 °C. 20 grams of pre-oxidized graphite was added over 460 mL of concentrated H_2SO_4 and the mixture was homogenized in a Berzelius beaker in ice bath (t < 5 °C). To this mixture were slowly added 60 g of $KMnO_4$. After a few minutes, the Berzelius beaker was removed from the ice bath and was placed

on a magnetic stirring plate at 35 °C for 2 hours. After heating the mixture, 920 mL of distilled H_2O were added, and over 15 minutes the reaction was stopped by adding a large amount of distilled H_2O and 30% H_2O_2. The resulting mixture was decanted, filtered, and washed with 5% HCl and distilled H_2O until a neutral pH was obtained. The obtained powder was dried in air at 60 °C for 24 h.

In order to obtain the composites, during the synthesis of the magnetite by the precipitation method, the necessary quantities of GO prepared previously were added. Table 1 presents the mass composition of GO-Fe_3O_4 composites.

Table 1. The composition of GO-Fe_3O_4 composites

No.	*Sample Code*	*GO content (g)*	*Fe_3O_4 content (g)*	*Mass ratio*
1.	GM15	0.1	1.5	1:15
2.	GM10	0.1	1.0	1:10
3.	GM5	0.1	0.5	1:5
4.	GM1	0.1	0.1	1:1
5.	M	0	1.5	

2.2. Characterization methods

The microstructure of GO-Fe_3O_4 composites was assessed by Scanning Electron Microscopy (SEM) using a high-resolution electronic scanning microscope (FEI Inspect F50) with a resolution of 1.2 nm at 30 kV and 3 nm at 1 kV (BSE) and EDAX accessory.

The X-Ray diffraction analysis were performed at room temperature using a PANalytical Empyrean diffractometer with Cu Kα (λ= 0.154 nm) radiation, and the scanning was performed between $2\theta = 10$ and 80 degrees. Supplementary information was obtained by Raman analysis. To obtain the Raman spectra a LabRAM HR Evolution type instrument produced by Horiba was used, using a 633 nm laser and a 50x objective.

Thermal analysis was performed on a NETZSCH STA 490C instrument, in air, in the temperature range: 25 – 900°C with a heating rate of 10°C/min and the magnetic measurements were made at 25 ± 2°C using a 7400 Series VSM produced by LakeShore.

The catalyst efficiency was tested by measuring the absorbance intensity at 662 nm using a UV-VIS Evolution 300 Spectrometer, Thermo Scientific. The removal efficiency was calculated using the Equations (1) and (2):

$$Photodegradation\,rate = \frac{C_t}{C_0} \quad (1)$$

$$Removal\,efficiency = \left(1 - \frac{C_t}{C_0}\right) x\ 100 \quad (2)$$

3. Results and discussions

The obtained composites were analyzed by X-ray diffraction, the results being presented in Fig. 1. As can be seen, all the samples have a crystalline character, the diffraction peaks characteristic to the magnetite being easily identified in all the analyzed samples.

Table 2 presents the position of the maximum associated with the diffraction plane (311) as well as the average crystallite size calculated using the Debye-Scherrer Equation (3).

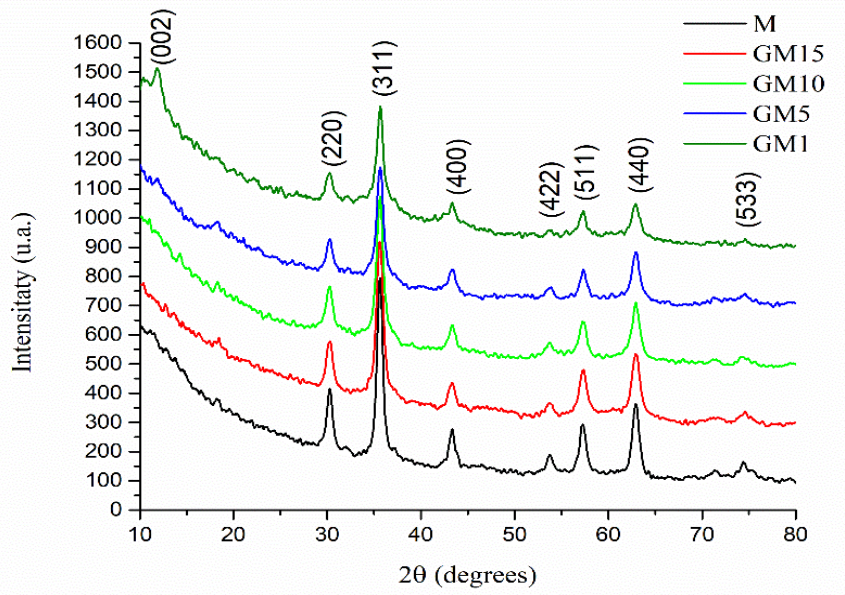

Fig. 2. XRD patterns for magnetite (M) and GO-Fe_3O_4

$$d = \frac{K\, x\, \lambda}{\beta\, x\, cos\, \theta} \qquad (3)$$

Table 2. The XRD parameters of samples

No.	*Sample Code*	*(311) position*	*d, Å*	*FWHM, 2q°*	*Crystallite dimension, nm*
1.	M	35.60	2.5197	0.70	9.9453
2.	GM15	35.59	2.5203	0.83	8.2275
3.	GM10	35.59	2.5200	0.82	7.6851
4.	GM5	35.60	2.5192	0.81	7.7806
5.	GM1	35.60	2.5191	0.90	6.9372

It is worth noting that with the increase of the GO content, a decrease in the intensity of the magnetite characteristic peaks is observed. Also, the presence of GO decreases the crystallite size from 9.9453 nm for simple magnetite to about 6.9372 nm when the ratio between the two components is 1:1. This can be attributed to the graphene sheets limiting the magnetite crystallization process.

Fig 2. presents the scanning electron microscopy (SEM) images for the GO-Fe_3O_4 composites, highlighting the nanometric size of the magnetite particles obtained. As can be observed, by the proposed synthesis method, magnetite with average particle size between 5 and 7 nm is obtained.

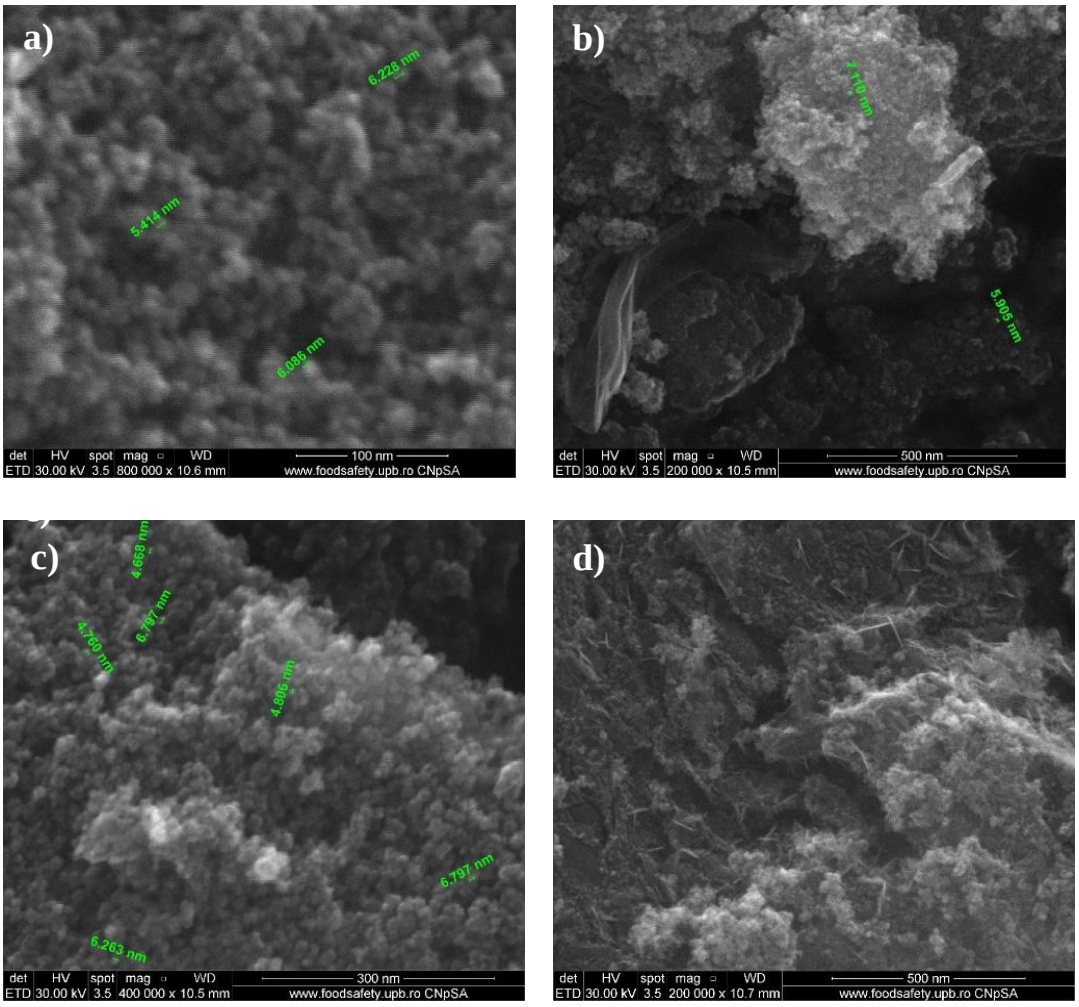

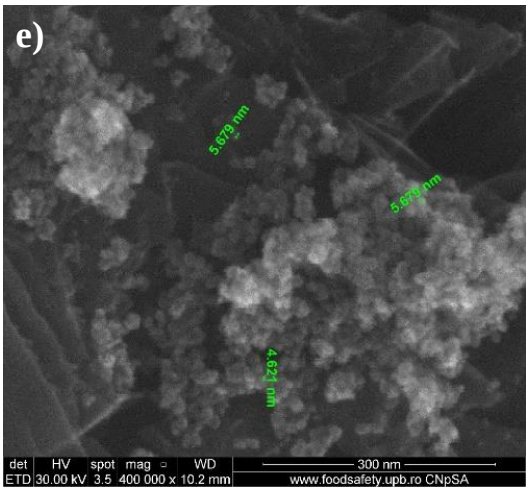

Fig. 4. SEM images for magnetite (a), GM15 (b), GM10 (c), GM5 (d) and GM1 (e).

With the addition of GO, the degree of agglomeration of these particles decreases, since graphene sheets might act as a coating for the magnetic nanoparticles, reducing their surface reactivity. When the ratio between the amount of GO and the amount of Fe_3O_4 was 1:1 (GM1), see Fig 2e, a good distribution of the magnetite particles on the graphene oxide sheets is observed, the tendency of this agglomeration being minimal. The reduced size of the nanoparticles and the maximum resolution of the equipment make it difficult to pinpoint the shape of the particles, which seems quasi-spherical.

In order to better understand the composition of composites, complex thermal analysis (TG and DTA) was performed on selected compositions (Fig. 3). The GO sample shows a mass loss of 9.76% in the range 25 °C - 130 °C. The process is accompanied by an endothermic effect, with a minimum at 91.9 °C, indicating a decomposition or evaporation. The sample may continue traces of solvent or weaker C-O bonds break within this range. The oxidation of the sample takes place energetically, in the range 130°C - 195 °C, when the sample loses 25.13% of the mass, the process being accompanied by a strong, sharp exothermic effect, with a maximum at 185.2 °C. This pyrolysis is specific to graphene oxide even if the atmosphere is inert, because it is made with the oxygen contained in it. Then there is a slower oxidation stage, in the temperature range of 195 °C - 310 °C, with a mass loss of 12.52% followed by one oxidation step with a mass loss of 5.64% in the temperature range 310 °C - 480 °C. The total oxidation of the carbon occurs after 480 °C, up to 660 °C, the loss of mass being 45.34%, the process being accompanied by a large exothermic effect, with two maxima at 560.8 °C and 629.2 °C (Fig. 3b).

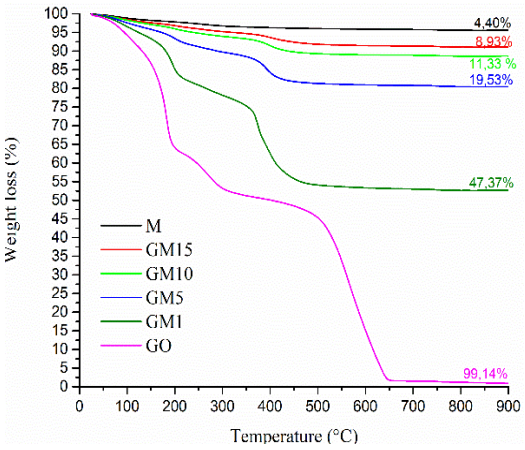

a. TG curves

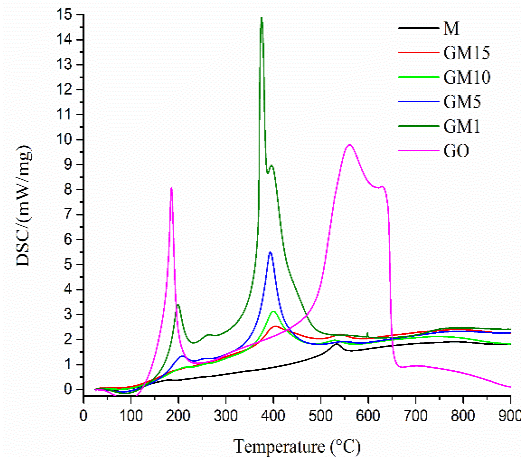

b. DSC curves

Fig. 5. Complex thermal analysis on magnetite (M) and GO-Fe_3O_4 composites

In the case of GO-Fe_3O_4, from GM1 to GM15, is observed that as the amount of GO decreases, the exothermic effect due to oxidation below 200 °C becomes very weak. The effect due to the burning of the carbon at around 400 °C decreases in intensity and it becomes wider as the amount of GO decreases. The effect of transforming maghemite into hematite becomes more visible as the amount of magnetite in the initial sample increases.

Raman spectroscopy is used to investigate the ordered and disordered crystal structures of carbonic materials, graphene, graphene oxide and reduced graphene oxide. Raman spectra of GO-Fe_3O_4 composite materials were presented in Fig. 4 and show the existence of D band around 1,336 cm^{-1}, which can be associated to the sp^3 defects, and the G band around 1,584 cm^{-1}, related to the in-plane vibration of sp^2 carbon atoms present in hexagonal lattice of graphene oxide [17,18].

The relatively high intensity of D band in all the samples, indicating the presence of localized sp^3 defects within sp^2 clusters during functionalization process of exfoliated GO [18]. As can be seen in Fig. 4, the Fe_3O_4 pure (M) shows a broad and strong peak centered at 685 cm^{-1} characteristics of magnetite, which is the symmetric stretch of oxygen atoms along Fe–O bonds (A1g). In addition, the bands at 209, 262, 365 and 484 cm^{-1}, correspond to the A1g(1), Eg2, Eg3, Eg4 and A1g(2), modes of hematite The presence of magnetite bands in the spectra, along with those of hematite, is explained by the stability of magnetite nanocrystals with respect to oxidation by laser power during Raman measurements [19].

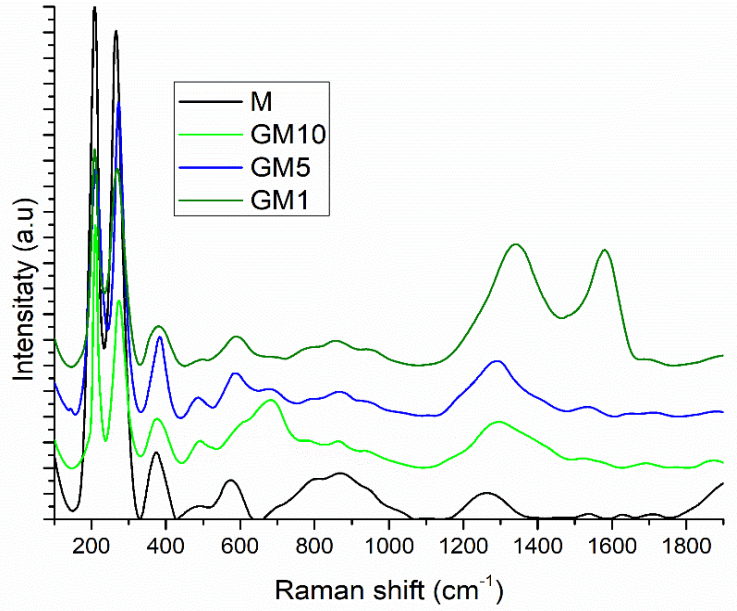

Fig. 6. Raman spectra for magnetite (M) and GO-Fe_3O_4

In order to verify the magnetic behavior of the samples, the magnetization variation according to the magnetic field at 25° C applied for the composite samples and the simple magnetite was analyzed by VSM measurements. As can be seen in Fig. 5, the obtained materials have a super-paramagnetic character demonstrated by the S-shape of the obtained curves. The saturation magnetization is shown in Table 3. This is between 19.18 emu/g and 84.26 emu/g and decreases with the decrease of Fe_3O_4 content in the composite materials, saturation magnetization being a linear function of the nanoparticle diameter value [20].

Table 3. The saturation magnetization of the samples

No.	*Sample Code*	*Magnetization, emu/g*
1.	GM15	59.35
2.	GM10	52.75
3.	GM5	41.51
4.	GM1	19.19
5.	M	84.26

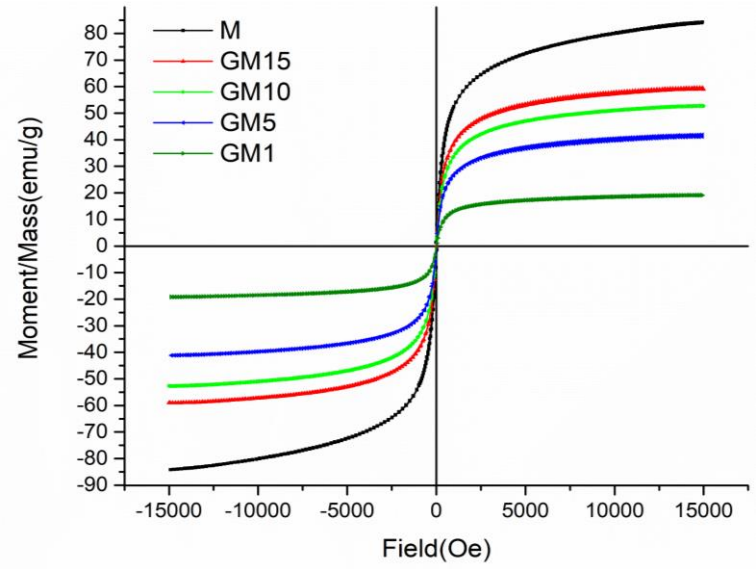

Fig. 8. VSM magnetization curves of magnetite (M) and GO-Fe_3O_4.

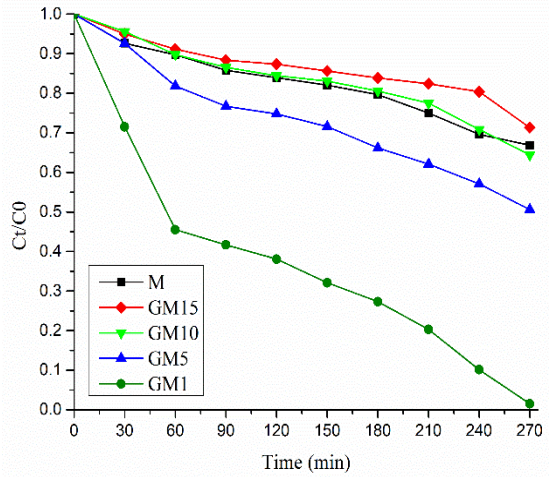

a. The photocatalytic degradation of methylene blue

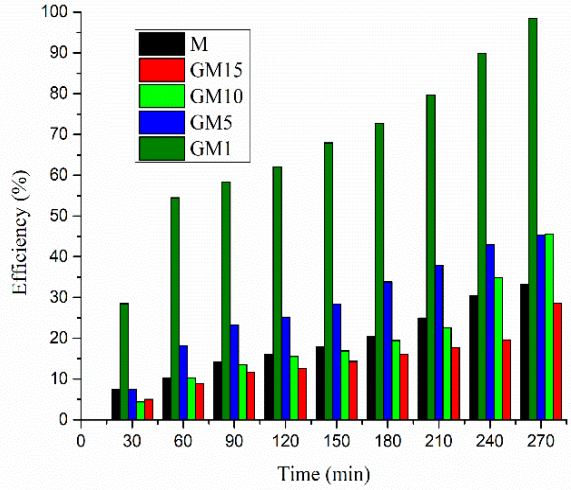

b. The photocatalytic efficiency of the degradation of methylene blue.

Fig. 9. The photocatalytic degradation of methylene blue under sunlight irradiation

The photodegradation studies show that the most efficient nanocomposite is GM1, which has a ratio of GO to Fe_3O_4 of 1:1. As can be seen in Fig 6.b, after 270 min this composite reduces the concentration of the dye completely while the other composites with a higher content of Fe_3O_4 reach only 50% efficiency at the same time interval.

The reduced size of the magnetite particles in the composition of this sample can be associated with a large specific surface which causes an increased reactivity to methylene blue, which makes the composite effective in treating polluted waters with various industrial dyes.

Conclusions

Our study proposed to use an economic and environmental-friendly photocatalysts based on magnetically separable GO-Fe_3O_4 nanocomposites to remove methylene blue at room temperature. For characterizing the material, various morphological and structural analysis techniques such as XRD, SEM, Raman and ATD were used. The behavior in the magnetic field was evaluated with the VSM technique obtaining a high value of the saturation magnetization and a low coercivity, which demonstrates the superparamagnetic behavior of the magnetite. The photodegradation studies show that the most efficient nanocomposite is GM1, which has a ratio of GO to Fe_3O_4 of 1:1, after 270 min this composite reduces the concentration of the dye completely while the other composites with a higher content of Fe_3O_4 reach only 50% efficiency at the same time interval.

Acknowledgment

Adrian Ionut NICOARA, Alexa Croitoru and Ionela Andreea NEACSU highly acknowledge the grant received from Academy of Romanian Scientists.

R E F E R E N C E S

[1] R. Tang *et. al.*, Removal of Methylene Blue from Aqueous Solution Using Agricultural Residue Walnut Shell : Equilibrium , Kinetic , and Thermodynamic Studies (2017).

[2] A. Nezamzadeh-ejhieh, H. Zabihi-mobarakeh, *J. Ind. Eng. Chem*. **20**, 1421–1431 (2014).

[3] A. Sudhaik *et. al.*, *J. Ind. Eng. Chem.* **67**, 28–51 (2018).

[4] P. Shandilya, D. Mittal, M. Soni, P. Raizada, *J. Clean. Prod.* **203**, 386–399 (2018).

[5] A. Nezamzadeh-Ejhieh, M. Bahrami, *Desalin. Water Treat.* **55**, 1096–1104 (2015).

[6] P. Janos, H. Buchtova, M. Ryznarova, *Water Res*. **37**, 4938–4944 (2003).

[7] A.G. Espantaleon, J.A. Nieto, M. Fernandez, A. Marsal, *Appl. Clay Sci.* **24**, 105–110 (2003).

[8] K.S.P. Kalyani *et. al.*, *Chem. Eng. J.* **151,** 1–3 (2009).

[9] A.N. Kagalkar *et. al.*, *Bioresour. Technol.* **100,** 4104–4110 (2009).

[10] S.B. Jadhav *et. al.*, *Int. Biodeterior. Biodegrad*. **65**, 733–743 (2011).

[11] B. Li, Y. Hao, X. Shao, *J. Catal.* **329**, 368–378 (2015).

[12] A. Thiam *et. al.*, *Appl. Catal. B Environ*. **180**, 227–236 (2016).

[13] D.K. Gardiner, B.J. Borne, *J. Soc. Dye. Colour*. **94,** 339–348 (1978).

[14] T. Peik-See *et. al.*, *Catal. Sci. Technol.* **4**, 4396–4405 (2014).

[15] J. Shekhovtsova, M. Kovtun, E.P. Kearsley, *Adv. Cem. Res*. **28**, 3–12 (2016).

[16] A. Croitoru *et. al. Medicina* **55**, 230 (2019).

[17] M. Zong *et. al.*, *Rsc Adv.* **3**, 23638–23648 (2013).

[18] L. Ren, S. Huang, W. Fan, T. Liu *Appl. Surf. Sci.* **258**, 1132–1138 (2011).

[19] O.N. Shebanova, P. Lazor, *J. Raman Spectrosc.* **34**, 845 (2003).

[20] X. Liua *et. al., Compos. Part A Appl. Sci. Manuf.* **89**, 40–46 (2016).